Operated for NASA by AURA

Instrument Science Report WFC3 2012-15

The WFC3 IR "Blobs" Monitoring

N. Pirzkal, B. Hilbert
Nov 13, 2012

ABSTRACT

We present new results on the WFC3 IR "Blobs" based on analysis of data acquired using the WFC3 IR channel from 2010 to 2012. In particular, we trace the date of appearance of each of the Blobs we identified in our deep IR sky flats. The number of Blobs identified in the WFC3 IR channel is now 40, and increase of a factor of 2 from our earlier 2010 ISR. We also discuss the color of the blobs, as measured using the F105W, F125W and F160W filters. We find Blobs to be more opaque to bluer light and their effect is therefore slightly stronger in the F105W and F125W filters when comparing these to the F160W filter. We find that the IR Blobs have appeared during somewhat discrete events and that there was a period a little over one year long when no new Blobs appeared.

Introduction

Small blemishes, or "Blobs", were identified in WFC3 IR images following the successful installation of WFC3 on board of HST in May 2009. We reported on Blobs in Pirzkal et al. (2010) and at that time we identified 19 distinct Blobs. We have carried on with the routine analysis of WFC3 IR datasets and have monitored the stability of existing blobs and the appearance of new ones. The analysis described in this ISR relies on the creation of deep sky-flats (Pirzkal et al. 2011), following the same methodology that was described in Pirzkal et al. (2010). We now have a much larger data pool from which to construct deep sky flat-fields. As more data became available, higher signal-to-noise sky-flats could be created, as well as sky-flats covering particular periods of time, allowing us to find these Blobs. The measurements presented in this ISR were performed on deep sky-flats that were generated using data between the dates of 2010-01-01 and 2012-07-01.

New Blobs

As shown in Figure 1, IR blobs continue to affect the WFC3 IR channel. Moreover, when comparing the number of Blobs shown in Figure 1 to Figure 5 in Pirzkal et al. (2010), a significant number of new blobs are visible. All 19 blobs identified in 2010 are still visible and have not been observed to physically move on the detector.

Table 1 lists a set of blobs that we have identified. Many of these are shallow and absorb less than 1% of incoming light. The WFC3 IR Bad Pixel Map was updated and delivered to CDBS (w681807ii_bpx.fits) on June 8, 2012.

Table 1: List of blobs identified in the deep WFC3 IR sky-flats. Coordinates are given for a reduced UVIS FLT file (1024x1024 pixels). We give date estimates (MJD 55000 is June 18, 2009) with associated error in cases where we were able to fit a step function to the F125W and F160W data. The errors listed are the standard deviation computed from fitting the F125W data, the F160W data. and fitting simultaneously the F125W and F160W data. In cases where error is indicated the date listed is the average of these three estimates. In cases were no error is given, the date listed is the result of a visual inspection of the data.

X coordinate	Y coordinate	Radius (pixel)	F105W	F125W	F160W	Date (MJD)
7	657	8	0.981 +/- 0.016	0.979 +/- 0.017	0.988 +/- 0.021	55813.4 +/- 1.0
20	223	10	0.983 +/- 0.007	0.982 +/- 0.009	0.986 +/- 0.027	55000
22	844	4	0.993 +/- 0.022	0.992 +/- 0.025	0.999 +/- 0.040	55200
46	7	8	0.933 +/- 0.009	0.937 +/- 0.010	0.955 +/- 0.017	<55071
83	618	6	0.988 +/- 0.015	0.991 +/- 0.026	0.989 +/- 0.022	55515.5 +/- 28.7
101	863	6	0.995 +/- 0.011	1.000 +/- 0.013	1.010 +/- 0.014	<55043

X coordinate	Y coordinate	Radius (pixel)	F105W	F125W	F160W	Date (MJD)
128	966	10	0.912 +/- 0.007	0.913 +/- 0.011	0.935 +/- 0.009	55207.9 +/- 20.4
210	167	9	0.979 +/- 0.010	0.986 +/- 0.024	0.990 +/- 0.024	55850
228	418	12	0.886 +/- 0.005	0.888 +/- 0.008	0.918 +/- 0.007	55517.2 +/- 19.2
248	773	6	0.952 +/- 0.015	0.955 +/- 0.024	0.964 +/- 0.019	55814.9 +/- 8.9
252	649	6	0.985 +/- 0.015	0.984 +/- 0.018	0.988 +/- 0.021	55400
259	505	10	0.944 +/- 0.019	0.944 +/- 0.011	0.941 +/- 0.014	55750
290	640	6	NA	0.939 +/- 0.019	0.951 +/- 0.021	<55043
302	45	9	0.970 +/- 0.008	0.973 +/- 0.015	NA	55068.0 +/- 29.5
315	386	9	0.967 +/- 0.008	0.967 +/- 0.010	0.979 +/- 0.010	<55043
321	993	4	0.956 +/- 0.024	0.967 +/- 0.028	0.971 +/- 0.057	55150
350	756	10	0.930 +/- 0.006	0.928 +/- 0.007	0.943 +/- 0.008	NA
406	81	11	NA	NA	0.971 +/- 0.012	55100
431	288	8	0.980 +/- 0.013	0.933 +/- 0.013	0.948 +/- 0.014	55866.3 +/- 3.3
438	919	6	0.965 +/- 0.014	0.952 +/- 0.016	0.967 +/- 0.018	55250
469	376	10	NA	0.927 +/- 0.011	0.950 +/- 0.013	55175

X coordinate	Y coordinate	Radius (pixel)	F105W	F125W	F160W	Date (MJD)
506	621	7	0.960 +/- 0.015	0.963 +/- 0.018	0.968 +/- 0.028	55800
548	64	7	0.972 +/- 0.016	0.968 +/- 0.017	0.979 +/- 0.019	55813.8 +/- 1.9
564	699	9	0.953 +/- 0.008	0.957 +/- 0.009	0.959 +/- 0.012	<55043
564	836	3	0.995 +/- 0.047	1.000 +/- 0.065	1.001 +/- 0.070	NA
567	828	4	0.985 +/- 0.025	0.981 +/- 0.028	0.981 +/- 0.033	55300
583	878	4	0.979 +/- 0.019	0.977 +/- 0.022	0.995 +/- 0.023	<55043
606	613	8	0.954 +/- 0.008	0.952 +/- 0.009	0.966 +/- 0.010	<55059
606	874	7	0.950 +/- 0.011	0.948 +/- 0.012	0.959 +/- 0.014	<55043
676	903	7	0.956 +/- 0.013	0.958 +/- 0.016	0.966 +/- 0.019	55150
778	334	5	0.945 +/- 0.022	0.943 +/- 0.028	0.958 +/- 0.031	55800
822	667	8	0.953 +/- 0.007	0.953 +/- 0.009	0.965 +/- 0.012	<55043
863	835	5	0.978 +/- 0.017	0.975 +/- 0.020	0.985 +/- 0.023	<55043
877	327	7	0.908 +/- 0.010	0.910 +/- 0.013	0.924 +/- 0.014	<55043
864	40	6	0.986 +/- 0.011	0.984 +/- 0.014	0.989 +/- 0.014	<55043
963	139	8	NA	0.962 +/- 0.015	0.973 +/- 0.019	55125

X coordinate	Y coordinate	Radius (pixel)	F105W	F125W	F160W	Date (MJD)
966	630	5	0.938 +/- 0.017	0.939 +/- 0.021	0.956 +/- 0.022	<55043
968	572	10	0.960 +/- 0.007	0.959 +/- 0.007	0.970 +/- 0.013	<55043
1000	593	8	0.969 +/- 0.008	0.970 +/- 0.009	0.974 +/- 0.011	55103.9 +/- 15.1
1001	659	4	0.968 +/- 0.024	0.968 +/- 0.024	0.985 +/- 0.033	55797.8 +/- 1.1

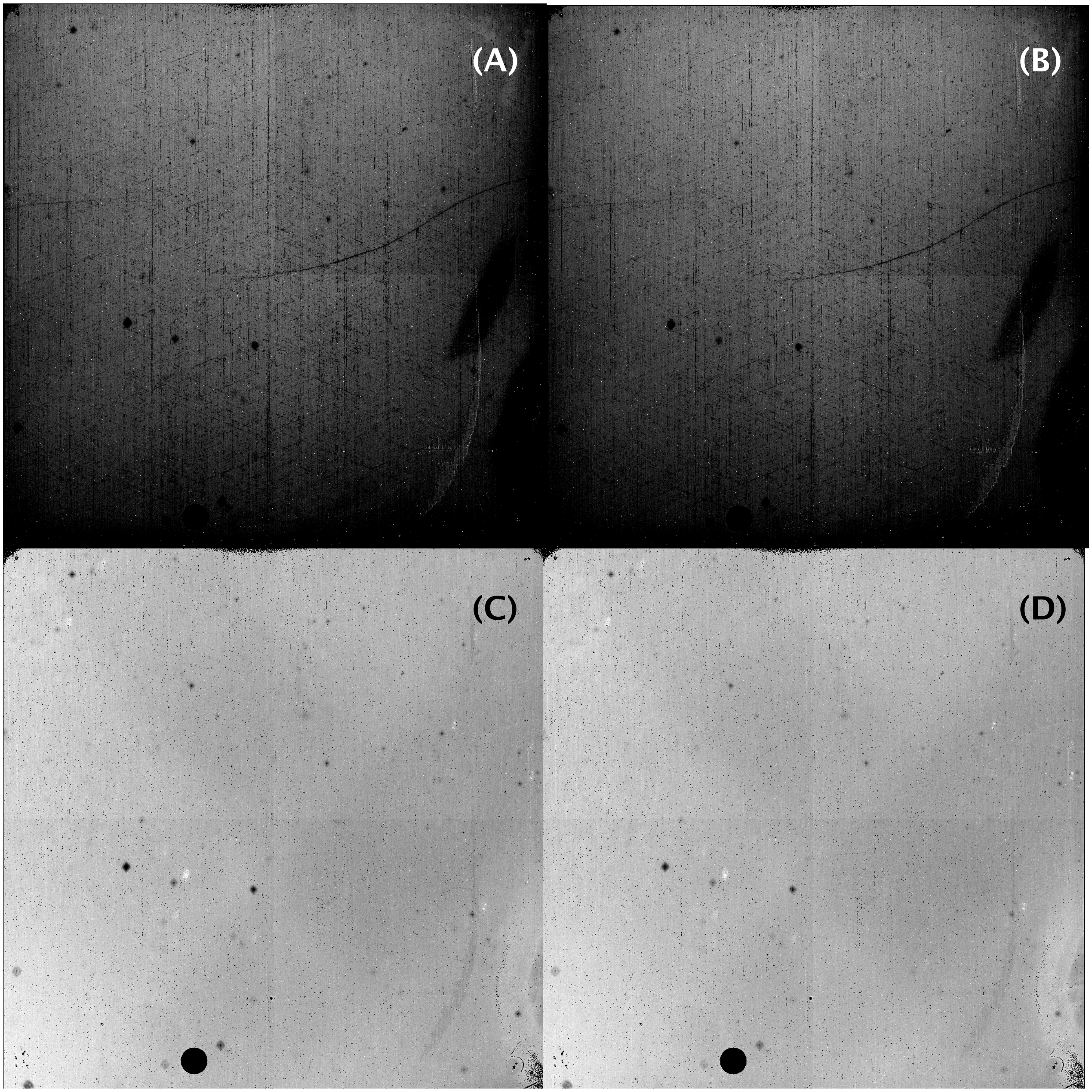

Figure 1: F125W (A) and F160W (B) sky flats assembled from available WFC3 IR data taking between 08-2010 and 06-2012. The same images but flat-fielded using ground flats to remove the large scale variations of the flat-fields are shown in the bottom two panels. A number of blobs, which appear as small darks dots, are visible in all images. When comparing these to Figure 5 of ISR WFC3 2010-06, a number of new blobs are clearly visible. Note that the “Deathstar”, the dark circular feature at the bottom left of the array is not a blob and is a known defect of the WFC3 IR detector.

Timelines

The same data that were used to construct the deep sky-flats used to detect blobs can be used to determine the approximate date when blobs appeared. Knowing the position of a blob, we simply performed aperture photometry at that position on every individual dataset used to construct the sky-flat. We used an aperture radius size of three pixels and normalized the result by the average sky level in the annulus between 5 and 10 pixels away from the center of the blob. While noisy, a clear and sudden decrease in sensitivity allowed us to identify an approximate start time for each blob; Figure 2 illustrates the results for the blob at pixel 248,773. We examined the timeline of each of the blobs listed in Table 1 and visually estimated the appearance date of most blobs. For some of the strongest blobs we fitted a step function to the timelines obtained using the F125W and the F160W data individually, as well as together, to derive three estimates

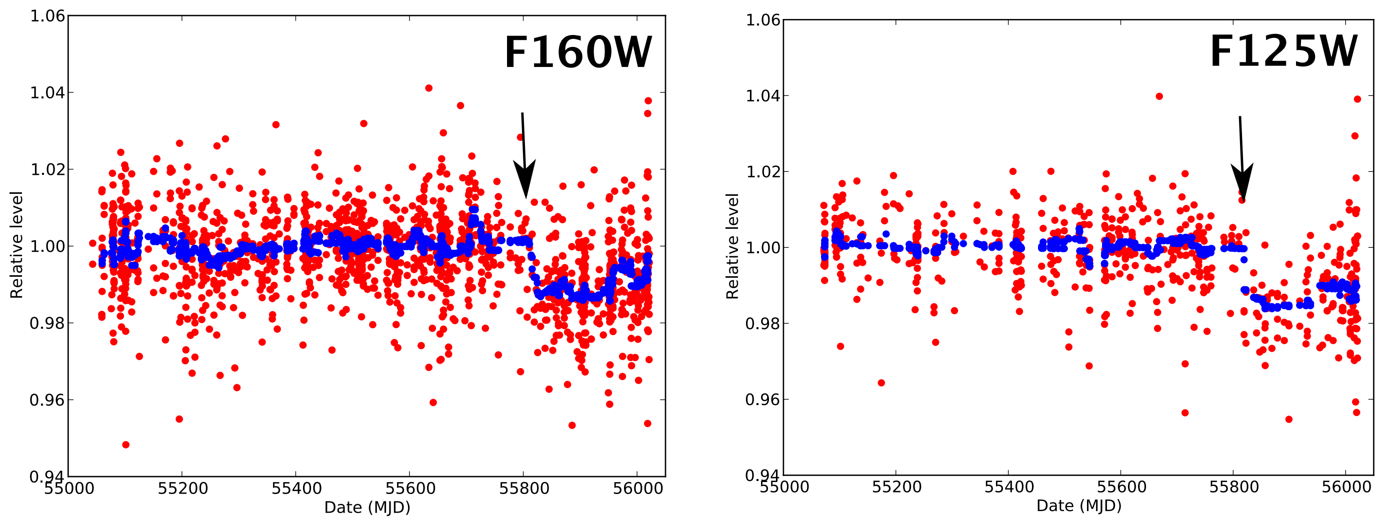

Figure 2: Timeline for the blob located at (248,773). The individual measurements are plotted in red and a smooth version is plotted in blue. The left and right panels show the F160W and F125W timeline, respectively. The black arrow marks the approximate date at which this particular blob appeared. Both the F160W and F125W show the same drop in sensitivity at about the same time and we estimate this blob to have appeared on MJD=55814.9 +/- 8.9 (within 9 days of September 10, 2011).

of when the blob appeared. An average appearance date and its associated standard deviation were computed. Table 1 lists our estimates of the appearance date of blobs (in modified julian date, MJD, where MJD=55000 corresponds to June 28, 2009). As this Table also shows, most blobs appear to have been in place prior to our earliest observations (MJD~55000, ~June 2009).

Furthermore, plotting the accumulative number of blobs as a function of date (see Figure 3) shows that the rate at which blobs appear has not been constant. We note that we find no instance of a blob having disappeared or moved once it was detected. Following the installation of WFC3

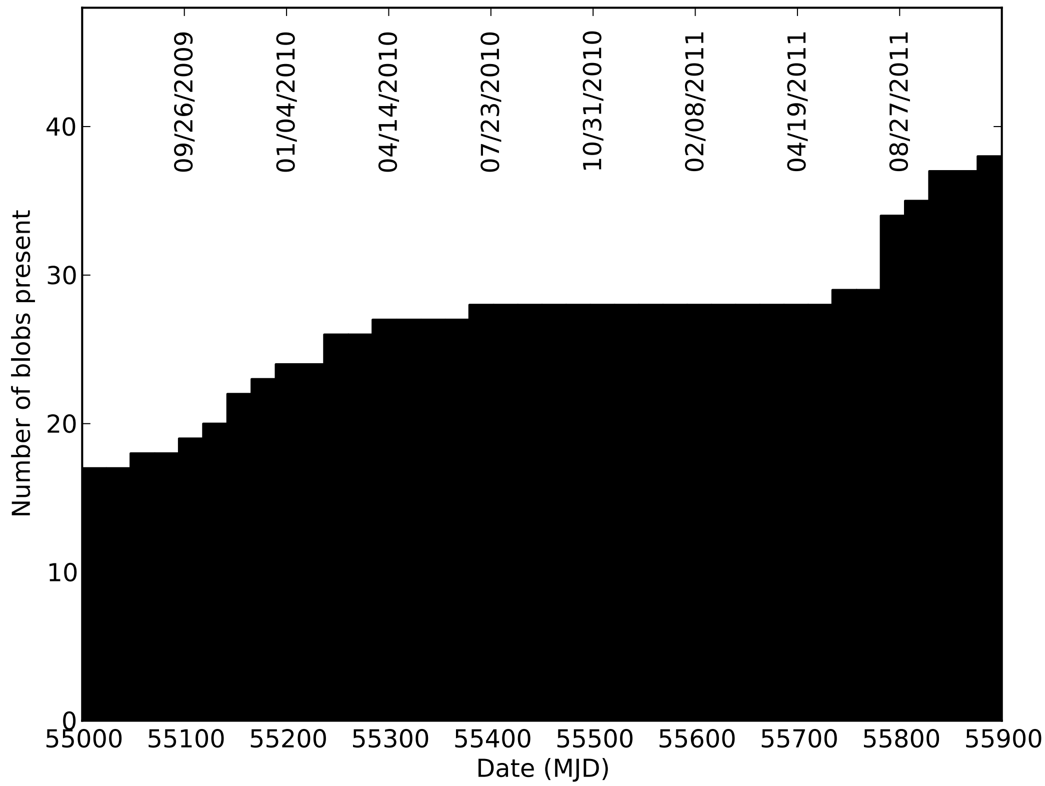

Figure 3: Plot of the number of blobs as a function of time (date in MJD). After the initial population of blobs was identified following the installation of WFC3 on board HST, the number of blobs increased at a constant rate for a few months before remaining constant for over one year (MJD ~55400 to ~55800, ~July 2010 to August 2011). We identified approximately 10 new blobs which appeared between MJD ~55800 and 55900 (August 2011 to December 2011), an increase of nearly 50% in the total population.

in June 2009 (MJD~55000) and up until April 2010 (MJD ~55300), the number of blobs increased slowly, at a rate of ~1 new blob per month. No new blobs were found between April 2010 and September 2011 (MJD~55800), when a handful suddenly appeared. Since then, the blob growth rate has been back to ~1 per month.

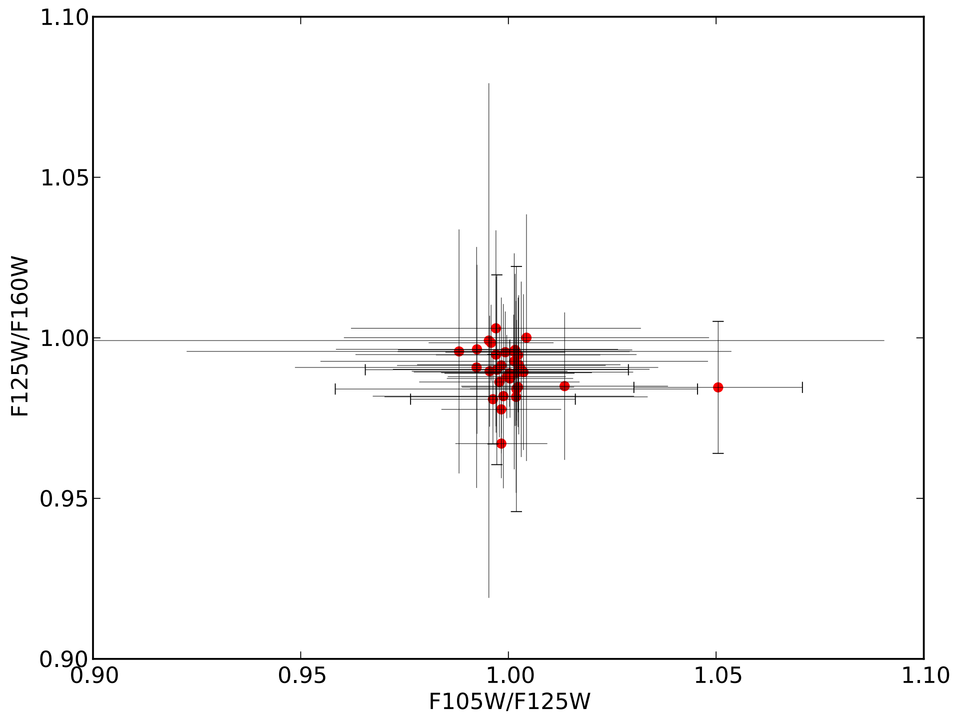

Figure 4: The ratio of the transmission (fraction of the light that is not absorbed by the blobs) in the F105W, F125W and F160W filters. Blobs appear to be more opaque in the bluer filters than in the redder filters.

Color dependence of blobs

Once we determined the date at which a blob appeared, a high signal-to-noise image of the blob could be created by stacking all the data available following that date. We thus created images of the known blobs using available data in the F105W, F125W and F160W filters (the three filters where most data are available). Performing aperture photometry on the blob, using apertures with the radii listed in Table 1, we computed the transmission of each blob in the F105W, F125W and F160W filters. These measurements are included in Table 1. We assessed the "colors" of the blobs by computing the F105W/F125W and F125W/F160W transmission ratio. Figure 4 shows a plot of these "colors", including our error estimates of these measurements. The blobs appear to be slightly deeper (e.g. absorbing more of the incoming light) in the F125W filter rather than the F160W filter and to be statistically identical in the F105W and F125W filters. We compute an average F105W/F125W value of 1.0010 +/- 0.0046 and an average F125W/F160W value of 0.9896 +/- 0.0056.

Future Work

We are currently monitoring IR Blobs using dark Earth limb observations (Proposal 13099). These observations provide high background level images which are ideal to detecting and imaging Blobs. Regular Earth limb observations should provide us with the means to detect the appearance of Blobs more efficiently than the current sky flat-field based method.

References

Pirzkal N., Viana A., Rajan A. *The WFC3 IR "Blobs"*, ISR WFC3 2010-06

Pirzkal N., Mack J., Dahlen T., Sabbi E. *Sky Flats: Generating Improved WFC3 IR Flat-fields*, ISR WFC3 2011-11